Development 129, 5289-5300 (2002)

DEV2855

growth arrest specific gene 1 acts as a region-specific mediator of the *Fgf10*/*Fgf8* regulatory loop in the limb

Ying Liu[1], Chunqiao Liu[1], Yoshihiko Yamada[2] and Chen-Ming Fan[1,*]

[1]Department of Embryology, Carnegie Institution of Washington, Baltimore, Maryland 21210, USA
[2]Craniofacial Developmental Biology and Regeneration Branch, NIDCR, National Institutes of Health, Bethesda, Maryland 20892, USA
*Author for correspondence (e-mail: fan@ciwemb.edu)

Accepted 21 August 2002

SUMMARY

Proximal-to-distal growth of the embryonic limbs requires *Fgf10* in the mesenchyme to activate *Fgf8* in the apical ectodermal ridge (AER), which in turn promotes mesenchymal outgrowth. We show here that the *growth arrest specific gene 1* (*Gas1*) is required in the mesenchyme for the normal regulation of *Fgf10*/*Fgf8*. *Gas1* mutant limbs have defects in the proliferation of the AER and the mesenchyme and develop with small autopods, missing phalanges and anterior digit syndactyly. At the molecular level, *Fgf10* expression at the distal tip mesenchyme immediately underneath the AER is preferentially affected in the mutant limb, coinciding with the loss of *Fgf8* expression in the AER. To test whether FGF10 deficiency is an underlying cause of the *Gas1* mutant phenotype, we employed a limb culture system in conjunction with microinjection of recombinant proteins. In this system, FGF10 but not FGF8 protein injected into the mutant distal tip mesenchyme restores *Fgf8* expression in the AER. Our data provide evidence that *Gas1* acts to maintain high levels of FGF10 at the tip mesenchyme and support the proposal that *Fgf10* expression in this region is crucial for maintaining *Fgf8* expression in the AER.

Key words: *Gas1*, *Fgf8*, *Fgf10*, Limb, Growth, Apical ectodermal ridge, Mouse

INTRODUCTION

In vertebrates, limb buds are formed from the lateral plate mesoderm by an early induction from the adjacent somites and intermediate mesoderm (Harrison, 1921) (reviewed by Stocum and Fallon, 1982). The limb mesoderm then induces the overlying ectoderm to thicken and form the apical ectodermal ridge (AER) (Zwilling, 1961). The AER in turn provides signals that drive limb outgrowth (Saunders, 1948) along the proximodistal (PD) axis. The signals responsible for these activities have been assigned molecularly (reviewed by Martin, 1998). *Fgf8* expressed in the somitic and intermediate mesoderm is presumed to be the limb bud initiation signal (Crossley et al., 1996; Vogel et al., 1996); it consolidates the expression of *Fgf10* in the lateral plate mesoderm to the prospective limb domains (Ohuchi et al., 1997). *Fgf10* in the limb mesenchyme then induces the AER-specific *Fgf8* expression (Ohuchi et al., 1997; Min et al., 1998; Sekine et al., 1999). *Fgf8* in the AER in turn maintains *Fgf10* expression in the mesoderm (Mahmood et al., 1995; Vogel et al., 1996; Ohuchi et al., 1997; Moon and Capecchi, 2000). *Fgf4*, *Fgf9* and *Fgf17* are expressed in the posterior AER and likely join forces with *Fgf8* to act upon the mesenchyme (Lewandoski et al., 2000; Sun et al., 2002). The *Fgf8*/*Fgf10* regulatory loop thus fulfills the documented mutual interactions between the mesenchyme and the AER to stimulate limb outgrowth and generate the appropriate amount of cellular mass for the formation of all the limb skeletal elements.

There are many modulators of AER function. *Shh*, expressed in the zone of polarizing activity (ZPA), regulates *Fgf4* in the posterior AER by acting through the intermediate component Gremlin, a BMP inhibitor (Zuniga et al., 1999). Inhibition of BMP signaling also can increase the thickness of the AER (Pizette and Niswander, 1999). These studies indicate that BMP negatively modulates AER function and that SHH counteracts this by modulating the BMP signal. However, at an earlier stage, BMP signaling is necessary for AER formation (Ahn et al., 2001; Pizette et al., 2001). *Fgf10* appears to act through the *Wnt/β-catenin* pathway in the ectoderm to activate *Fgf8* in the AER (Kawakami et al., 2001). Consistently, the null mutant mouse embryos of *Tcf1* and *Lef1*, the *Wnt* downstream mediators, do not express *Fgf8* in the AER (Galceran et al., 1999). FGFs from the AER serve to maintain *Fgf10* expression in the mesenchyme, but whether they are the sole and direct input or require additional modulators and intermediate components is not yet known.

Sufficient mesenchymal mass is required for the formation of the skeletal elements of the appropriate number and size. The aforementioned growth regulators are important in the generation of a defined amount of mesenchymal mass. From this will be produced the mesenchymal condensations representing the limb skeletal elements, including the proximal

segment (stylopod; femur/humerus), the medial segment (zeugopod) with two elements (tibia-fibula/radius-ulna), and the distal segment (autopod) with, in the mouse, the five elements (digits) (Hinchliffe and Griffiths, 1983; Shubin and Alberch, 1986). These skeletal elements arise by endochondral cartilage formation, starting with a group of mesenchymal cells that condense and differentiate into chondrocytes (Erlebacher et al., 1995). The growth and size of each element are then coordinately regulated by successive transitions in differentiation that are locally controlled, for example, through the activities of BMP and of IHH, which activates a negative feedback relay system by regulating PTHrP (a negative growth regulator) (Ganan et al., 1996; Vortkamp et al., 1996; Zou et al., 1997; St-Jacques et al., 1999).

We have previously proposed that GAS1, a GPI-anchored membrane glycoprotein (Stebel et al., 2000), acts as an inhibitor of SHH via direct physical interaction (Lee et al., 2001a). However, *Gas1* mutant mice do not display phenotypes related to those of SHH overexpression (Lee et al., 2001b; Liu et al., 2001). Instead, we report here that *Gas1* mutant limbs have defects caused by reduced proliferation in the AER and mesenchyme, and develop with small autopods, missing phalanges and anterior digit syndactyly. We provide several lines of experimental evidence supporting the model that *Gas1* is a necessary mesenchymal factor that positively regulates *Fgf10* in a regional- and temporal-specific manner to maintain the *Fgf10/Fgf8* regulatory loop.

MATERIALS AND METHODS

Gas1$^{-/-}$ mice

Gas1 mutant mice were described previously (Lee et al., 2001b). After backcrossing to CD1 and to 129sv females for five successive generations, the mutant limb defects remained in both backcrosses. For this study, animals used were from the CD1 backcrosses because the mutants were viable in this background. PCR was used to determine the genotype (Lee et al., 2001b).

Skeletal preparation

Skin and internal viscera were removed and the bodies fixed overnight by St. Marie's fluid, followed by standard Alcian Blue and Alizarin Red staining procedures (Bancroft and Cook, 1994). Whole-mount fetal Alcian Blue staining was performed according to the same protocol omitting the Alizarin Red.

In situ hybridization (ISH)

ISH on paraffin sections (8 μm) with ^{35}S-UTP-labeled probes was performed as described previously (Fan and Tesseir-Lavigne, 1994). Photographs of the detected transcripts were taken as dark-field images with a red filter. Phase images were taken with a blue filter and overlayed with the dark-field images. Whole-mount ISH using DIG-labeled probes was performed following standard procedures (Wilkinson, 1992). Probes used were: *Gas1* (Lee and Fan, 2001), *Shh* (gift from Dr McMahon), *Fgf8* (gift from Dr Martin), *Fgf4*, *Gli3* (gift from Dr Hui), *Fgf9*, *Fgf17* (gift from Dr Ornitz), *Bmp2*, *Bmp4*, *Bmp7* (gift from Dr Hogan), *Gremlin* (gift from Dr Zeller), *Hoxb8*, *Hoxd13* (gift from Dr Duboule) and *Alx4* (gift from Dr Wisdom).

BrdU and TUNEL assays

Mice were injected with 10 mg/ml BrdU (Sigma) at 0.01 ml/g body weight, 1 hour before sacrifice. BrdU-positive cells were detected by using a BrdU staining kit (Zymed). Cell death assays were performed using the In Situ Cell Death Detection Kit, Fluorescein (Boehringer Mannheim) according to the manufacture's protocol.

In vitro limb culture

Embryonic limbs were cultured as described previously (Zuniga et al., 1999). E9.75-E11.5 embryos from heterozygous mating were dissected in L-15 medium. The heads and tails were removed for genotyping and the trunks including forelimbs were used for injection. Recombinant FGF10 and FGF8 proteins (Research Diagnostic Inc.) resuspended in PBS were delivered by glass needles. 1-25 μg/ml of FGF10 and 1-100 μg/ml of FGF8 were used for injection and a pulse of 9.2 nl was injected into the right forelimb mesenchyme underneath the AER. The left forelimb was not injected and served as an internal control. Mock injection was performed using PBS. The injected limb buds were cultured in BGJb medium with 0.2 mg/ml ascorbic acid (Gibco/BRL) at 37°C/5% CO_2. After overnight culturing, the trunk fragments were fixed and subjected to whole-mount ISH.

RESULTS

Gas1 mRNA exhibits a dynamic expression pattern in the developing limb

The mouse *Gas1* transcript is detected in the early limb bud (Lee and Fan, 2001; Lee et al., 2001c). Here we extend the documentation by whole-mount and section in situ hybridization (ISH). At E9.25 and E9.5, *Gas1* is expressed in the entire lateral plate mesoderm and in the forelimb bud (Fig. 1A,B). It is preferentially expressed in the anterior part of the limb mesenchyme. This asymmetric pattern continues to E10.5 (Fig. 1C) and is also observed in the hindlimb (not shown). Sections through various planes of the limb bud indicate that *Gas1* is expressed in approximately the anterior two-thirds of the mesenchyme. Adjacent sections of an E10.5 forelimb hybridized to *Gas1* and *Fgf8*, an AER marker, confirm that *Gas1* is expressed up to the distal tip of the mesenchyme abutting the anterior-to-central AER but not in the AER (Fig. 1H). At E11.5, *Gas1* expression retains its anterior preference and apparently corresponds to the mesenchymal condensations of the radius and ulna (Fig. 1D). At E12.5, *Gas1* is expressed in the condensing mesenchyme and the interdigital mesenchyme (Fig. 1E,I) (Lee and Fan, 2001; Lee et al., 2001c). One day later, it is expressed at the outer edges of the condensed digital rays, the prospective joints, and weakly in the interdigits (Fig. 1F,J) (Lee and Fan, 2001; Lee et al., 2001c). From E14.5 to E15.5, its transcripts are restricted to the perichondrium, the articular surface and the joints (Fig. 1G,K). Its mesenchymal expression pattern suggests its role in limb growth, patterning and/or skeletogenesis.

Gas1 mutant mice have limb abnormalities

To define the role of *Gas1* in limb development, we analyzed the limb phenotype of *Gas1* null mutant (*Gas1*$^{-/-}$) mice (Lee et al., 2001b). Newborn *Gas1*$^{-/-}$ mice have smaller fore- and hind-limb paws (Fig. 2A-B'). Skeletal preparation using the dyes Alcian Blue (for cartilage) and Alizarin Red (for calcified bone) revealed that this is due to a size reduction of all phalanges, metacarpals and metatarsals (Fig. 2C-D'). The calcified regions were of normal size but the chondrogenic regions were reduced in proportion. Digits I-III were disproportionately reduced in size. In addition, the second phalange of digit II was greatly reduced (Fig. 2C') or absent

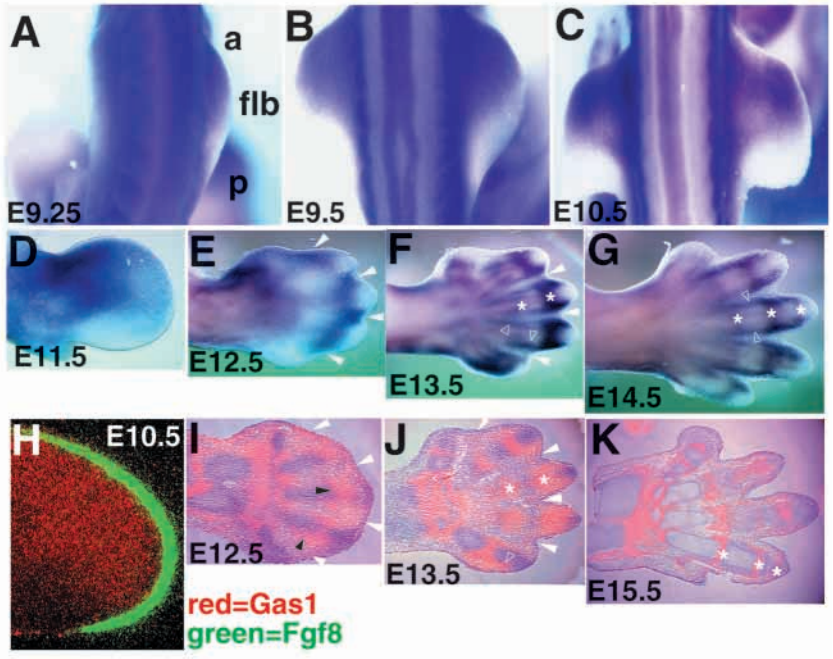

Fig. 1. *Gas1* transcripts are detected in developing limbs. Expression of *Gas1* was examined by ISH. (A-C) Dorsal view of the forelimbs at E9.25, E9.5 and E10.5. Anterior (a) is at top and posterior (p) at bottom; flb, forelimb bud. *Gas1* is expressed in the lateral plate mesoderm and asymmetrically in the limbs with higher levels anteriorly. (D-G) Whole-mount ISH of E11.5-E14.5 forelimbs shows expression in the autopod (dorsal view, anterior at top). White arrowheads indicate the interdigital regions; open arrowheads, perichondorgenic regions; asterisks, joints or prospective joints. (H-K) ^{35}S-ISH of E10.5-E15.5 forelimbs (horizontal sections, anterior at top). (H) Superimposed images from adjacent sections of E10.5 *Gas1* expression (red) in anterior two-thirds of the mesenchyme but not in AER (visualized by *Fgf8* expression (green) in the adjacent section). At E12.5 (I), *Gas1* transcripts (pink granules) are prominent in the prechondrogenic region (black arrowheads) and the interdigits (white arrowheads). At E13.5 (J), *Gas1* is expressed in the interdigits (much weaker than at E12.5) and prospective joints (asterisks). At E15.5 (K), *Gas1* is localized to perichondrium lining the joint cavities (asterisks).

(Fig. 2D'), and there was a high rate of soft tissue fusion between digits II and III (Fig. 2A',B'). Syndactyly between digits II and III was also observed by histology (Fig. 2D') and by X-ray imaging (not shown). The frequency of these defects is summarized in Fig. 2E. The front and hind paws of the adult *Gas1*$^{-/-}$ mice were almost of normal size (not shown), indicating a compensatory growth postnatally. Carpals, tarsals and long bones (radius, ulna, tibia, fibula) were either slightly shorter or not affected. Macroscopic and histological analyses revealed no apparent defects in the patterns of muscles and tendons (not shown). Thus, *Gas1* contributes to proper formation of the autopodial skeletal elements, in particular the phalangeal elements and the anterior digits.

The *Gas1* mutant has a delay in digit formation

We next determined the ontogeny of the mutant phenotype by histology (Fig. 3). As early as E11.5, the mutant limb bud width across the AP axis is noticeably reduced (Fig. 4B'). The prechondrogenic condensations of digits II-IV in the forelimb are normally visible by E12.5 (Fig. 3A). In the mutant, condensations of digits III and IV are smaller and digit II is less evident (Fig. 3A'); the autopod is also narrower along the AP axis and shorter along the PD axis. At E13.5, the metacarpals and first phalange are individualized by the onset of joint formation (Fig. 3B). In the mutant, separation of the phalanges is ill-defined and the phalanges of digit II and metacarpal I are not apparent (Fig. 3B'). From E13.75 to E14.5, the third and second phalanges of all digits become clearly defined (Fig. 3C,D); whereas in the mutant, the second phalanges of digits II and III are not individualized (Fig. 3C',D').

At E16.5, ossification of metacarpals III and IV is delayed in the mutant (Fig. 3E,E'). At E17.5, ossification of the first phalanges of digits III and IV (Fig. 3F,F') is clearly delayed. While ossification of digit III second phalange is delayed by about 24 hours, digit II second phalange does not appear to ever ossify (Fig. 3F' and not shown). Intriguingly, as soon as the ossification assumes, the bone segments appear normal in size at the expense of the chondrogenic domains (Fig. 2C', Fig. 2D', Fig. 3F'). The mutant hindlimb phenotype is similar (Fig. 2E). These manifestations suggest that *Gas1*$^{-/-}$ limbs have reduced mesenchymal mass as early as E11.5, which at least in part leads to the small and delayed condensations. Delayed or absent joint formation may affect the size of the chondrogenic region, but *Gas1* is not essential for chondrogenic differentiation.

Reduced cell proliferation in the AER and distal mesenchyme in *Gas1*$^{-/-}$ limbs

To detect alterations in cell proliferation, we assayed bromodeoxyuridine (BrdU) incorporation in vivo. At E10.5, the rate of BrdU incorporation in the limb mesenchyme adjacent to the AER (cells within 150 μm of the AER were counted and compared) was not altered in the mutant (Fig. 4A,A'). Note that the mutant AER is present but thinner than normal. AER morphology was confirmed by scanning electron microscopy (not shown). Importantly, the mutant AER has fewer BrdU^{+} cells (Fig. 4A',D), indicating a non cell-autonomous effect of *Gas1* on the AER. The most marked difference in the mesenchymal proliferation rate is observed at E11.5 (Fig. 4B,B',D). The reduction is observed preferentially in the distal mesenchyme at the anterior-to-central portion of the mutant limb: mild anteriorly and severe in the central region (Fig. 4D). This cellular mass reduction prefigures the delay in digit formation. When the digit ray is visible at E12.5, we found no marked difference in the rate of proliferation between digit III/IV and digit IV/V of mutant and control limbs. However, between digit II/III, there was a significant reduction (~10%) in proliferation rate in the mutant (Fig. 4C,C',D). This regional-specific defect is surprising given the more general *Gas1* expression in all interdigits at this stage. These findings suggest that the main proliferation defect occurs around E11.5 and the perduring smallness of the embryonic limb is due to this early deficiency of precursor population.

Programmed cell death (PCD) is reduced in the *Gas1*$^{-/-}$ limb

PCD is found in the following areas of the developing chick limb: anterior and posterior necrotic zones, the opaque patch, the interdigital mesenchymes and the joints (Hinchliffe, 1982; Hurle et al., 1996). *Gas1* expression overlaps with the opaque patch at E11.5, the interdigits at E12.5-13.5 (albeit weakly), and the joints (E13.5-E15.5) (see also Lee and Fan, 2001; Lee et al., 2001c). Furthermore, overexpression of *Gas1* can trigger PCD in cultured limb mesenchymal cells (Lee et al., 2001c). To assess whether *Gas1* normally plays a role in PCD, we performed TUNEL-fluorescence labeling. At E11.5, fewer apoptotic cells were detected in the central mesenchyme area (opaque patch) in the mutant compared to control forelimb (Fig. 5A,A'), even though the limb is already smaller. In the control E13.5 forelimbs, cell death was observed in the interdigital zones and the prospective joints of the digits (Fig. 5B). Interdigital cell death in *Gas1*$^{-/-}$ forelimbs was relatively normal posterior to digit III but greatly reduced anterior to digit III (Fig. 5B'), correlating with the anterior soft tissue syndactyly. Joint PCD was delayed in digits II and III in the mutant, consistent with the delay in phalange separation seen histologically. Since the mutant limbs appear delayed in development, we also examined PCD at E14.0. There was still little PCD between digits II and III, but PCD appeared relatively normal between other digits (compare Fig. 5B,C,C'). By contrast, PCD in the mutant joints at this time appeared at a higher rate than those of the wild type at E13.5 and E14.0 (of digits II-IV in Fig. 5C').

Reduced PCD between digits II and III suggests that *Gas1* normally facilitates PCD and supports the claim by Lee et al. (Lee et al., 2001c), but in other interdigits, PCD appeared to be relatively normal. However, more apoptotic cells were detected in the mutant joints, suggesting that *Gas1* is anti-apoptotic. In other affected regions of the *Gas1* mutant, such as the eyes and the cerebellum (Lee et al., 2001b; Liu et al., 2001), the PCD rate is not altered. Either *Gas1* regulates PCD in a cell-context-dependent manner or these region-specific alterations of PCD are a secondary consequence of deregulated growth and heterochrony of the mutant limb.

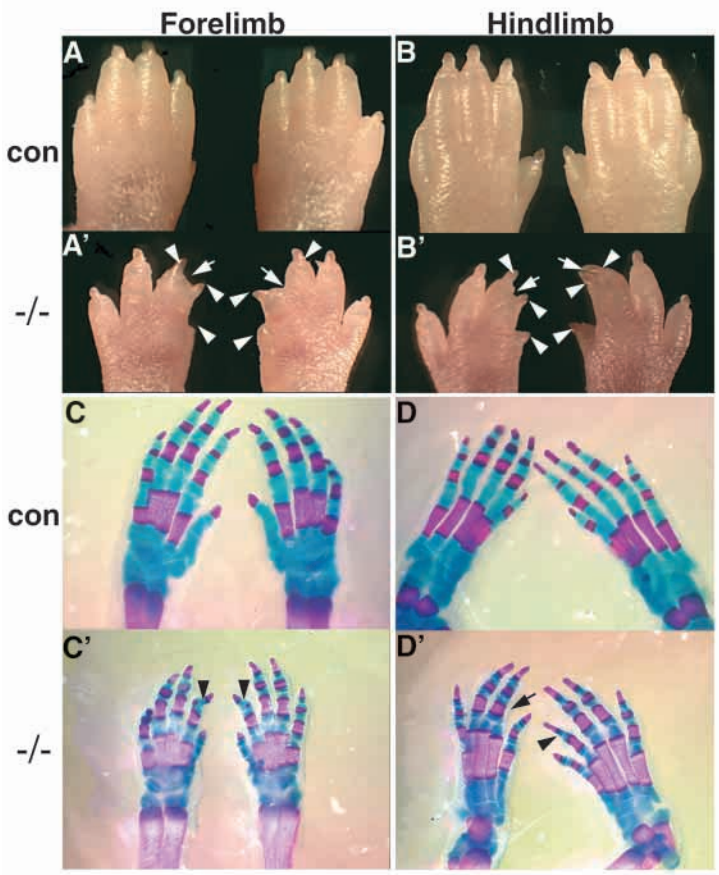

E. Summary of *Gas1* mutant limb phenotype*

Gas1$^{-/-}$	digit II phalange 2 reduced/missing	soft tissue syndactyly (digit II-III)	syndactyly (digit II-III)
Forelimbs	56/56**	41/56	13/56
Hindlimbs	56/56	45/56	18/56
Both	56/56	39/56	12/56

*All mutant limbs had small paws and their digits I-III were disproportionally reduced in size.

**56 mutant animals were examined. Visual examination was used to determine soft tissue syndactyly. Alcian blue-alizarin red skeletal preparation was used to determine the skeletal phenotype.

Fig. 2. *Gas1*$^{-/-}$ has limb abnormalities. Dorsal view of the newborn forelimb (A,A',C,C') and hindlimb (B,B',D,D') paws of a control (con; A-D) and a *Gas1* mutant (–/–; A'-D') animal. *Gas1*$^{-/-}$ forelimb and hindlimb paws are overall smaller and have syndactyly between digits II and III (A',B'). White arrows indicate soft tissue fusions and white arrowheads, disproportionally reduced digits. (C-D') Skeleton of the paws stained with Alcian Blue and Alizarin red. Black arrowheads indicate the reduction (C') or lack of (D') the second phalange of digit II; black arrows, syndactyly of digits II and III (D'). (E) A table summarizing the frequency of these skeletal defects in the *Gas1* mutants.

Expression of patterning genes is not obviously affected in the *Gas1*$^{-/-}$ limbs

Owing to the fact that GAS1 can physically interact with SHH and IHH (Lee et al., 2001a), we examined whether there are patterning abnormalities related to deregulated SHH signaling in the *Gas1* mutant, using a battery of functional marker genes in the SHH pathway. However, we did not observe expression pattern changes. *Shh* expression in the ZPA (Riddle et al., 1993; Echelard et al., 1993) was activated and maintained correctly at E10 and E10.5 (Fig. 6A' and not shown). *gremlin*, a downstream target of *Shh* (Zuniga et al., 1999), was expressed in the normal posterior domain albeit at apparently reduced levels (Fig. 6B'). The expression of *Bmp2* and *Bmp4* in the AER and the mesenchyme (reviewed by Hogan, 1996) was also apparently normal in positions and levels (Fig. 6C',D'). These results suggest that the thinner AER is not due to misregulation of *Bmps* or *gremlin*. Expression of *Ptc1* (*Ptch*) (Fig. 6E') (Marigo et al., 1996) and *Gli1* (not shown) (Hui et al., 1994) also appeared normal in the posterior domain. *Alx4* (Qu et al., 1997) and *Gli3* (Hui et al., 1994) expression was confined to the anterior domain in the mutant as in the control (not shown). These analyses were extended to E11.5 and E12.5 and no obvious alterations in these expression patterns were found. Lastly,

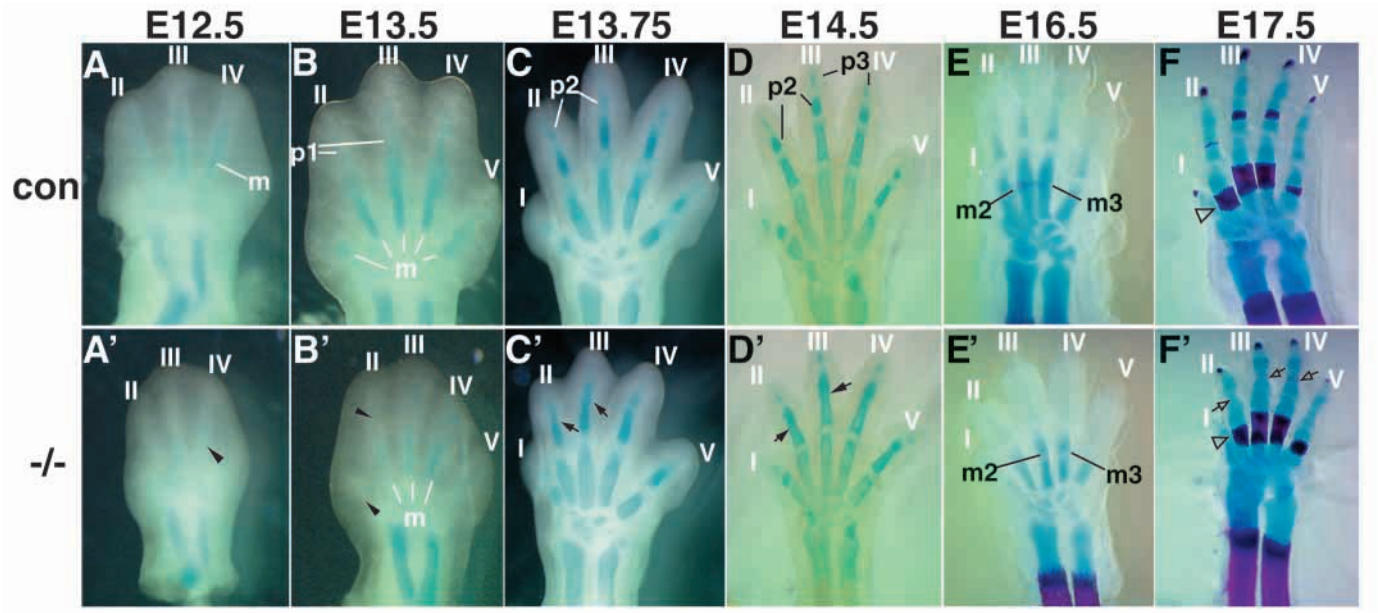

Fig. 3. *Gas1*$^{-/-}$ limbs display a delay in chondrogenesis and ossification. Whole-mount Alcian Blue (for cartilage) and Alizarin Red (for calcified bones) staining of control (con; A-F) and *Gas1*$^{-/-}$ (–/–; A'-F') embryonic limbs (dorsal view) at the indicated stages. In all panels, digit I is on the left, and digit V, on the right, as labeled. Arrowheads indicate delayed cartilage condensation (A',B'); arrows, delayed or lack of phalangeal separation (C',D'); open arrows, delayed ossification of the phalanges (F'); open arrowheads, the normal size of ossification of the metacarpals (F,F'); m, metacarpal; p, phalange.

Hoxd13 (Dolle et al., 1993) (Fig. 6F') and *Hoxb8* (Charite et al., 1994) (not shown) expression was activated at a normal distal position in the *Gas1*$^{-/-}$ limbs at E10.5 (not shown), E11.5 and E12.5 (not shown). The smaller domains of expression appear to be proportional to the smaller size of the limb bud.

Since in the mutant autopod chondrogenesis is delayed, we examined the expression patterns of *Ihh*, *Bmp2*, *Bmp4*, *Bmp7*, *BmpRIA*, *BmpRIB* and *PTHrP* (reviewed by Hogan, 1996) in the developing cartilage. Their expression was delayed corresponding to the delayed progression of the limb (by ~12 hours). Once initiated, these genes were expressed in normal patterns with proportionally smaller domains (data not shown). As *Gas1*$^{-/-}$ displays neither expanded nor reduced expression domains of *Shh* and *Ihh* downstream reporters and the *Gas1*$^{-/-}$ limb phenotype is unrelated to those of *Shh*$^{-/-}$ (Chiang et al., 2001) and *Ihh*$^{-/-}$ (St-Jacques et al., 1999), *Gas1* does not appear to modulate the activity of the hedgehog pathway in the limb.

Gas1 mutant limbs are defective in maintaining *Fgf8* expression

Because the *Gas1* mutant AER is thinner (Fig. 4A') and compromised AER function is a potential cause of reduced mesenchymal mass (reviewed by Martin, 1998), we reasoned that expression of the AER-specific *Fgf*s may be affected in the *Gas1* mutant. *Fgf4*, *Fgf9* and *Fgf17* expression in the AER at E10.5 (Fig. 7A-C) and E11.5 (not shown) was normal in the mutants when compared to the controls (not shown). In addition, *Fgf8* expression at E9.5 was also normally initiated (Fig. 7D,D'). However, at E10.0 and E10.5, AER-specific *Fgf8* expression was lost in the mutant (Fig. 7E',F'). At E11.5, variable small patches of *Fgf8* expression were regained in the mutant AER (Fig. 7G'). This *Fgf8* reappearance was restricted: when observed, it was most frequent in the posterior region, rarely in the anterior region, and never in the central AER. Loss of the FGF8 input from the AER may be the main cause of the *Gas1* mutant limb defects.

Fgf10 expression is reduced in the distal tip mesenchyme of the mutant limb

Fgf10 is necessary and sufficient to initiate *Fgf8* expression in the AER (Ohuchi et al., 1997; Min et al., 1998; Sekine et al., 1999). Whether it is continuously required to maintain *Fgf8* in the AER has not been established. It is possible that *Gas1* maintains *Fgf10*, which in turn maintains *Fgf8* in the AER. We therefore examined whether *Fgf10* expression is altered in the mutant. A small region of cells at the most distal tip mesenchyme immediately underneath the AER showed a clear absence of *Fgf10* expression at E9.5 both in the control and mutant forelimb (Fig. 8A,A'). At E10.0 and E10.5 (Fig. 8B,B',D,D'), *Fgf10* expression extended to the extreme tip of the control limb mesenchyme, whereas mutant cells located at the distal tip mesenchyme lacked *Fgf10* expression. This reduction of *Fgf10* expression could also be observed by whole-mount ISH (Fig. 8C',E'), but only in very few mutant limbs (~8% of the mutant limbs) – in these cases, the *Fgf10* loss appeared to be more extensive than that seen in sections. We reasoned that most mutants had a small affected domain (consistently detected by section ISH) which was not easily discerned by whole-mount ISH. Note that the anterior *Fgf10* expression domain was also slightly down regulated in the mutant. At E11.5, there was a moderate recovery of *Fgf10* expression in the mutant distal mesenchyme (Fig. 8F'), temporally corresponding to the reappearance of small patches of *Fgf8* expression in the AER. These results support a model in which *Gas1* is required to activate *Fgf10* expression in the

distal tip mesenchyme and *Fgf10* in this distal tip mesenchyme is crucial for maintaining *Fgf8* expression in the AER.

FGF10 injection restores *Fgf8* expression in *Gas1* mutant limb

In the above model, GAS1 deficiency should be overcome by supplementing FGF10 at the tip region. To test this, we applied FGF10 protein to the distal tip region of the *Gas1* mutant limb and examined restoration of *Fgf8* expression in the AER. The trunk segments containing the forelimbs of embryos between E9.75 and E11.5 were cultured using an in vitro system (Zuniga et al., 1999). At E9.75-E10.0 (*Fgf8* is already lost in the mutant AER), FGF10 protein ranging from 9.2 to 230 pg was delivered into the anterior-central mesenchymal tip region (where *Gas1* is normally expressed) underneath the AER, by microinjection. Only the right limb was injected, hence the left limb served as an internal control. The injected embryo trunks were cultured for 16 hours before harvesting for assessment of *Fgf8* expression (diagram in Fig. 9A). Injection of PBS into control (Fig. 9B) and mutant (Fig. 9E) right limbs did not alter their *Fgf8* expression when compared to the uninjected left side. Injection of 9.2 pg FGF10 protein (but not lower amounts) into the mutant right forelimb rescued *Fgf8* expression in the AER (Fig. 9F), while the uninjected side showed no *Fgf8* expression. At this amount of FGF10, only a weak and small domain of *Fgf8* expression was observed in the central AER of the mutant limbs. At 230 pg, FGF10 caused the entire length of the mutant AER to express high levels of *Fgf8* similar to the control limb injected with the same amount of FGF10 (Fig.

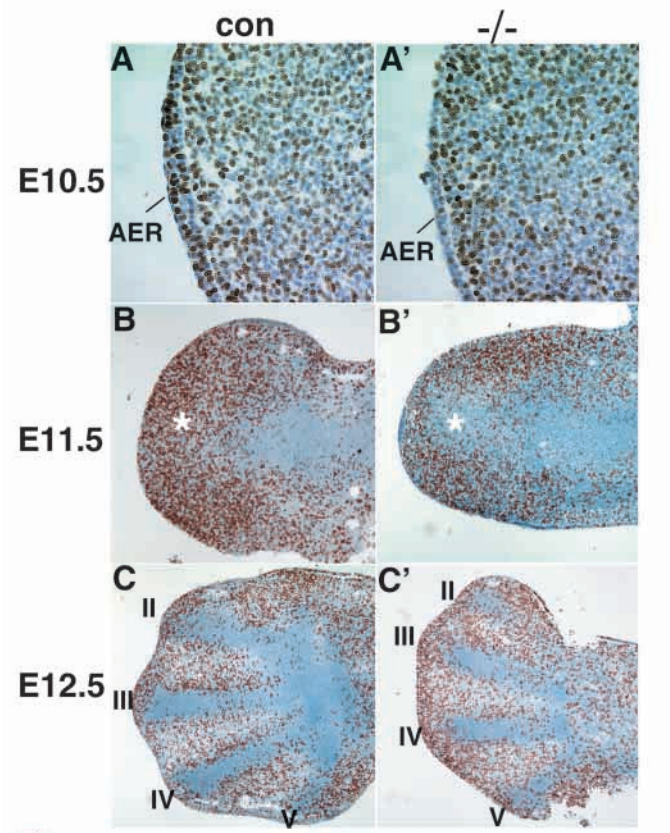

D. Cell proliferation rate in the AER, distal mesenchyme, and interdigital mesenchyme*

Age/Structure	Control	*Gas1-/-*	cells counted	*p* value (students t test)
E10.5 AER	54.1±2.7%	23.3±1.8%	120	< 0.001
E11.5 distal mesenchyme				
anterior 1/3	31.5±2.1%	27.1±1.5 %	1000	< 0.05
central 1/3	29.7±2.4%	17.8±2.3 %	1000	< 0.001
posterior 1/3	37.1±7.8%	34.9±1.6 %	1000	> 0.1
E12.5 interdigital				
between II and III	32.4±1.8%	22.3±4.7%	1500	< 0.001
between III and IV	21.7±5.6%	20.3±1.8%	1500	> 0.1
between IV and V	28.0±1.4%	29.4±2.2%	1500	> 0.1

* BrdU-positive cell counts are averages from three mutant and control forelimbs and shown as percentages of positive / total counted cells to represent the rate of proliferation.

Fig. 4. *Gas1*$^{-/-}$ limbs display defective cell proliferation in the AER and distal mesenchyme. In vivo BrdU labeling of control (con; A-C) and *Gas1*$^{-/-}$ (–/–; A'-C') embryonic forelimbs. (A,A') At E10.5, BrdU-positive cells were markedly reduced in the mutant AER. (B,B') At E11.5, BrdU-positive cells were reduced in the region of distal mesenchyme (asterisk) in *Gas1*$^{-/-}$. At E12.5, control (C) and *Gas1*$^{-/-}$ (C') have similar rates of cell proliferation in the interdigits between digits III/IV and IV/V, but reduced proliferation between digits II/III. Limbs were sectioned horizontally with the anterior at top. Note that the chondrogenic regions of digits III and IV have a lower rate of proliferation in the mutant (C'). (D) A table summarizing the BrdU counts of each stage.

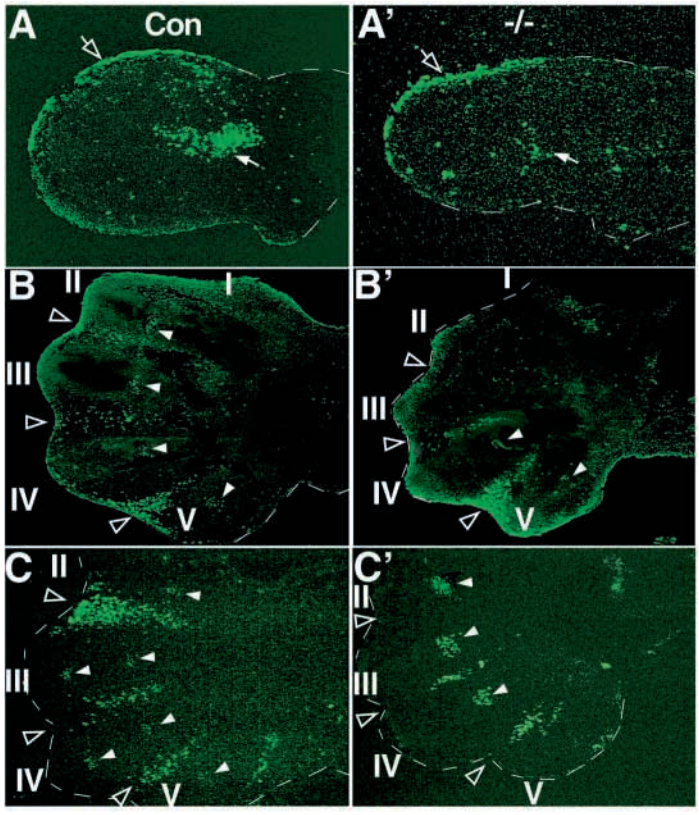

Fig. 5. *Gas1*$^{-/-}$ limbs have altered programmed cell death (PCD) patterns. PCD during limb development was assessed by TUNEL fluorescent labeling. In *Gas1*$^{-/-}$ (–/–), the TUNEL assay shows reduced and delayed PCD relative to control (con) at E11.5 (A,A'), E13.5 (B,B') and E14.0 (C,C'). White solid arrows indicate cell death at the opaque patch; white open arrows, the anterior margin; open arrowheads, the interdigital mesenchyme; white arrowheads, the forming joints. The limbs were sectioned horizontally and the digits are as labeled (I-V).

9D,G). There was also a FGF10 dosage-dependent increase in AER height in the injected mutant limbs. Notably, high levels of FGF10 injected into control limbs caused an increase in *Fgf8* expression as well as AER height compared to the uninjected side (Fig. 9D). At E11.5, after the *Fgf8* expression was lost for more than a day in the mutant, FGF10 injection still rescued its expression (Fig. 9I), indicating that *Fgf8* expression in the AER requires continuous input of FGF10. Injection of FGF10 to the proximal region (~200 μm from the AER) did not rescue *Fgf8* expression (not shown). Finally, injection of FGF8 protein (up to 1.8 ng) into the E9.75-E10.5 mutant limb did not rescue its own expression in the AER (Fig. 9J and not shown), suggesting that FGF8 cannot restore *Fgf10* expression at the distal tip. Thus, supplementation with FGF10, but not FGF8, at the distal tip mesenchyme can overcome the requirement of *Gas1*.

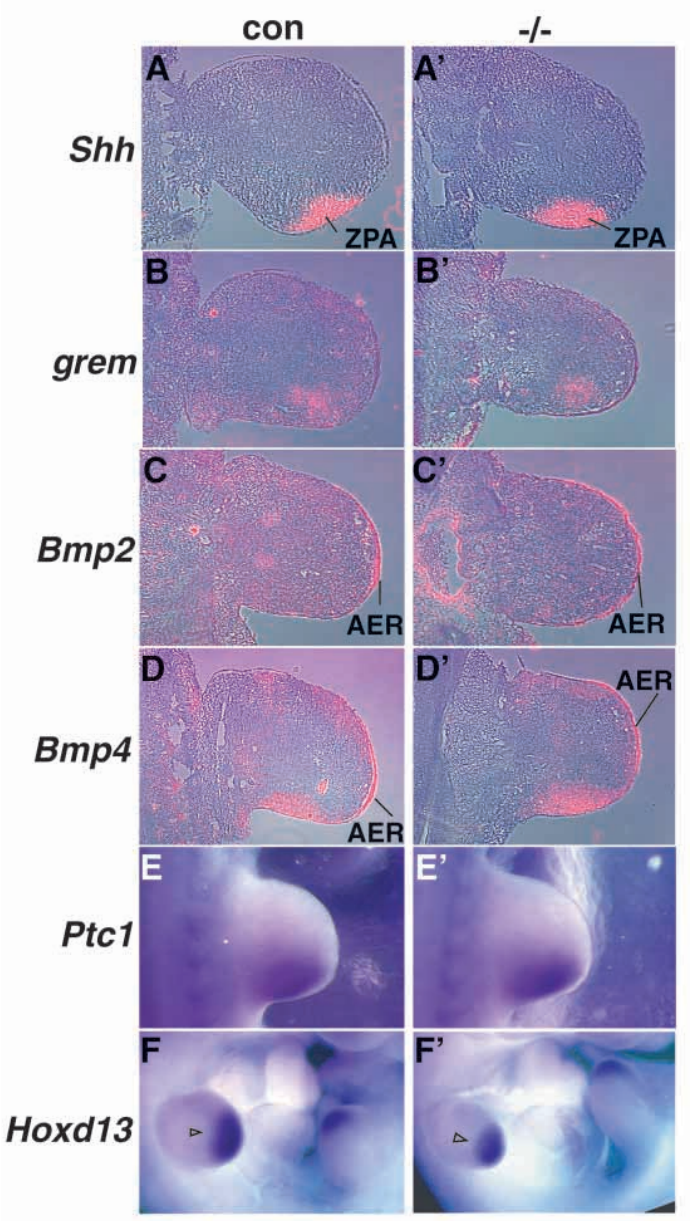

Fig. 6. Molecular analysis of *Gas1*$^{-/-}$ limbs for patterning genes. Control (con; A-E) and *Gas1* mutant (–/–; A'-E') forelimbs were compared for expression of *Shh*, *gremlin*, *Bmp2*, *Bmp4*, and *Ptc1* by ISH at E10.5. (A,A') *Shh* expression appears normal in *Gas1*$^{-/-}$ limbs. (C,C') *Bmp2*, (D,D') *Bmp4*, and (E,E') *Ptc1* expression is not obviously altered. (B,B') *gremlin* expression appears to be slightly reduced in the limb mesenchyme in the mutant. *Hoxd13* expression was examined at E11.5 (F,F') and found to be normal in the mutant – in a smaller domain proportional to the smaller size of the limb. Expression of *Ptc1* (dorsal view) and *Hoxd13* (lateral view, arrowheads indicate the forelimb expression) was assessed by whole-mount ISH; the others, by ^{35}S-ISH on horizontal sections with anterior at top.

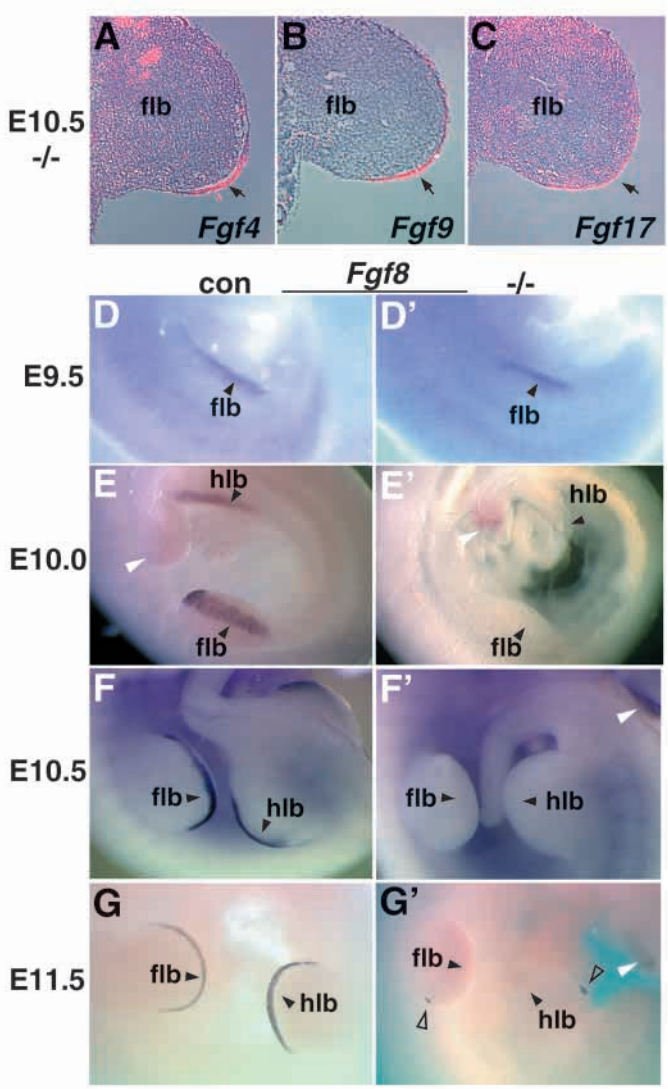

Fig. 7. ISH of *Fgf* expression in the *Gas1*$^{-/-}$ AER. (A-C) *Fgf4*, *Fgf9* and *Fgf17* gene expression (arrows) is normal in *Gas1*$^{-/-}$ limb at E10.5 as determined by ^{35}S-ISH on horizontal sections; anterior at top. Control (con; D-G) and *Gas-1*$^{-/-}$ (–/–; D'-G') collected at E9.5 (D,D'), E10.0 (E,E'), E10.5 (F,F') and E11.5 (G,G') were analyzed for *Fgf8* expression by whole-mount ISH. *Fgf8* expression is initiated but not maintained. Black arrowheads indicate the location of the AER; white arrowheads, *Fgf8* expression in other regions as an internal control (in the tailbud in E and E' and branchial arches in F' and G'); open arrowheads, reappearance of small patches of *Fgf8* expression in the posterior AER (G'); flb, forelimb; hlb, hindlimb.

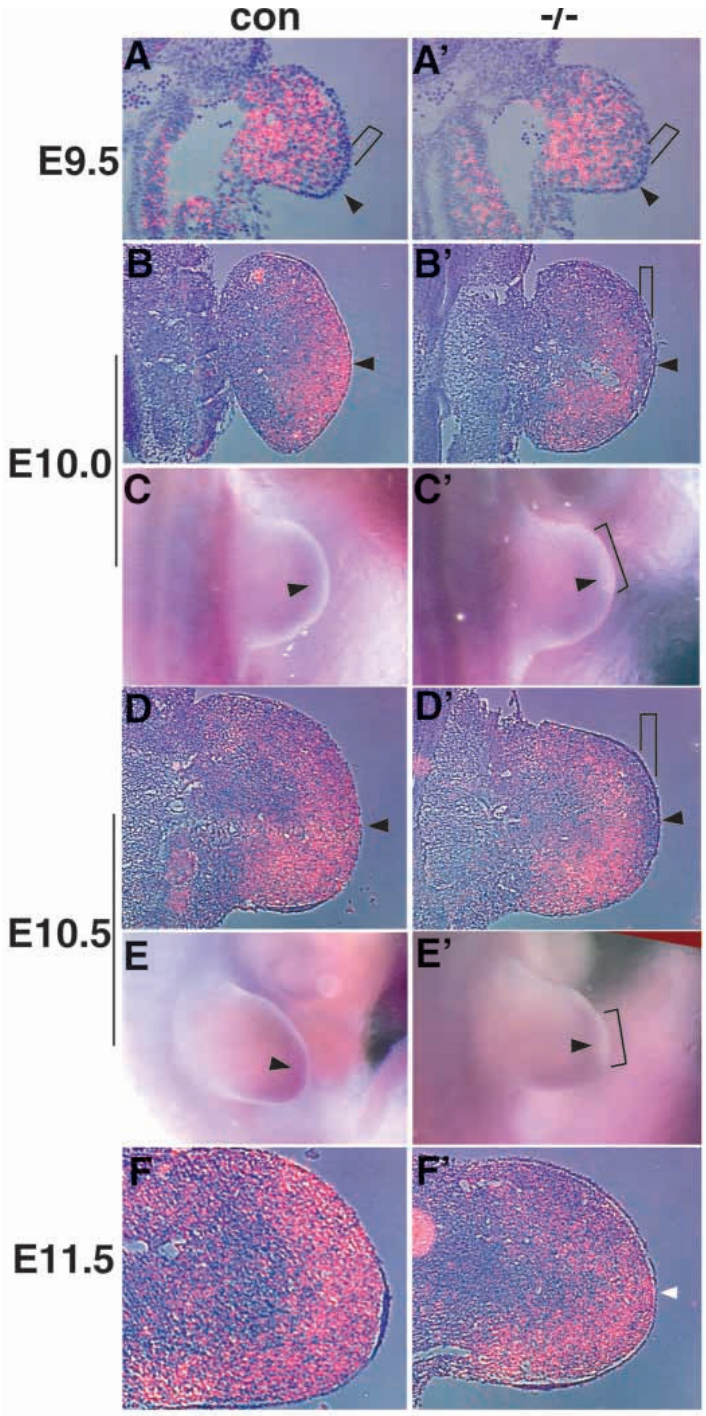

Fig. 8. Analysis of *Fgf10* expression in *Gas1*$^{-/-}$ limbs. *Fgf10* expression was detected by ^{35}S-ISH in control (con; A,B,D,F) and *Gas1*$^{-/-}$ (–/–; A',B',D',F') forelimb buds at E9.5, E10.0, E10.5 and E11.5 in horizontal sections (n=4). Arrowheads indicate the distal tip mesenchyme underneath the AER; brackets, the region of distal tip mesenchyme with reduced *Fgf10* expression in the mutant; white arrowhead, moderately recovered *Fgf10* expression at the distal region at E11.5. *Fgf10* expression was also assessed by whole-mount ISH in control (C,E) and *Gas1*$^{-/-}$ (C',E') forelimbs at E10.0 and E10.5 (dorsal and dorsal-lateral views, respectively). Only 2 out of 12 E10.0 and 2 out of 13 E10.5 embryos showed clear defects of *Fgf10* expression in one of the limbs by whole mount.

DISCUSSION

We report here the limb defects of the *Gas1* null mutant mouse. Deregulation of *Fgf10* in the mesenchyme and loss of *Fgf8* in the AER correlate with the proliferation defect and developmental delay of the *Gas1*$^{-/-}$ limb. Our data support a model in which *Gas1* acts as a novel regulator to maintain optimal levels of *Fgf10* in a previously unappreciated and specialized mesenchymal region to maintain *Fgf8* in the AER. These results provide several novel insights into limb development.

Gas1 plays a role in regulating proliferation of the developing limb through regulating *Fgf8* and *Fgf10*

Gas1$^{-/-}$ limbs display reduced proliferation preferentially in the anterior-to-central limb bud around E11.5. *Gas1* is normally expressed in the anterior-to-central region between E9.5-E11.5. Superficially, *Gas1* appears to be a cell autonomous positive regulator of proliferation. Paradoxically, *Gas1* overexpression is known to inhibit the cell cycle in cultured fibroblast (Del Sal et al., 1992). However, reduced proliferation in the *Gas1*$^{-/-}$ limb does not completely correlate with the time and pattern of *Gas1* expression. Reduced proliferation only became measurable after the *Fgf8* expression in the AER was lost, indicating that the proliferation defect is more likely the consequence of compromised AER function (reviewed by Johnson and Tabin, 1997). The preferential reduction in the anterior-to-central domain may reflect the fact that *Fgf4*, *9* and *17* are all expressed in their normal posterior AER domain, whereas *Fgf8* is lost throughout the AER and thus the anterior-to-central domain does not continue to receive the FGF signal. However, we cannot exclude the possibility that *Gas1* also directly contributes to anterior limb mesenchyme proliferation.

The mutant AER also has a decreased rate of proliferation. Our data suggest that *Gas1* acts indirectly to promote AER proliferation by establishing high levels of FGF10 at the distal tip mesenchyme. Consistently, injection of FGF10 at a high dosage can rescue the mutant AER such that it corresponds to wild-type AER in height and levels of *Fgf8* expression (Fig. 9G). This increase of AER height leads us to propose that FGF10 regulates not only the level of *Fgf8* expression in the AER but also the proliferation of the AER.

The continuous requirement of FGF10 for maintaining *Fgf8* expression in the AER

Both gain-of-function (Ohuchi et al., 1997) and gene inactivation studies (Min et al., 1998; Sekine et al., 1999) have provided evidence that *Fgf8* activation requires *Fgf10*. However, it was not clear whether *Fgf10* continues to be required to maintain *Fgf8* expression in the AER after initiation. The loss of *Fgf10*/*Fgf8* in the *Gas1*$^{-/-}$ limb and our FGF10 injection data in the *Gas1*$^{-/-}$ background strongly indicate that *Fgf10* at the distal region is continuously required for *Fgf8* expression and that the AER retains the potential to respond to FGF10 long after the loss of *Fgf8* expression.

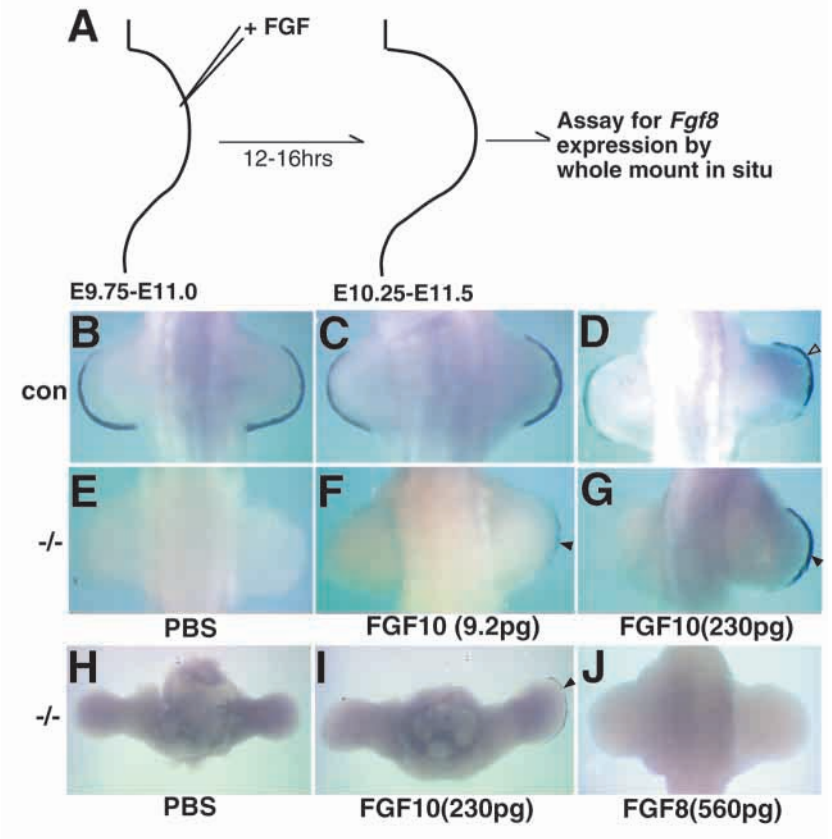

Fig. 9. FGF10 restores *FgF8* expression in *Gas1*$^{-/-}$ limbs. Mouse trunk fragments containing forelimbs were isolated from E9.75-E11.5 control (con; B-D) and mutant (–/–; E-G) embryos. (A) Diagram of FGF10 injection in anterior tip domain of the mesenchyme in the right limb. The injected embryo fragments were cultured for 16 hours and then subjected to whole-mount ISH to assay for *Fgf8* expression in the AER. (B,E) PBS-injected, (C,D,F,G) injected with recombinant human FGF10 protein: (C,F) 9.2 pg and (D,G) 230 pg. Note that in D and G, the color was developed for 20 minutes to reveal the upregulation of *Fgf8* in the injected wild-type limb (open arrowhead in D). The others were developed for 90 minutes. (J) Mutant E9.75 forelimb injected with 560 pg of FGF8 did not show any rescue of *Fgf8* expression in the AER. (H,I) Mutant E11.5 forelimbs were injected with PBS (H) or 230 pg of FGF10 (I). *Fgf8* expression in the AER was rescued in the FGF10-injected samples (arrowheads in F,G,I). Owing to the angle of the limbs relative to the body at this stage, the image was taken in a ventral view with the anterior pointing down. The control E11.5 limbs retained *Fgf8* expression in the AER after culture (not shown).

The *Gas1* mutant defines a domain of *Fgf10* in the distal tip mesenchyme required for *Fgf8* maintenance

Gas1 is required for *Fgf10* transcription at the distal tip mesenchyme of the limb between E10 and E11.5. Normally, from E10, *Fgf10* is expressed in a broad contiguous domain directly underneath and extending 150-200 μm away from the AER. In *Gas1*$^{-/-}$ limbs, *Fgf10* expression is lost in the distal-most 3-5 cell layers (or more cell layers in rare cases) next to the AER (Fig. 8B′-E′). In the chick, FGF8 or AER signals including a combination of FGFs induce *Fgf10* expression over a broad domain (Ohuchi et al., 1997). In *Gas1*$^{-/-}$ limbs, the proximal *Fgf10* domain is relatively normal (though weaker anteriorly), suggesting that the remaining AER FGFs can still act over a long distance. However, it also indicates that these remaining FGFs are not sufficient to maintain *Fgf10* at the distal tip, even though FGFRI expression is normal (including the tip region, not shown) in the mutant limb. Reciprocally, our data indicate that the distal tip *Fgf10* expression is necessary and sufficient, as shown by FGF10 rescue injection, to maintain *Fgf8*. Thus *Gas1* is necessary to maintain the distal *Fgf10* domain and this is required to maintain *Fgf8* expression in the AER.

This finding provides several novel insights (Fig. 10). First, there are two distinct regulatory mechanisms for *Fgf10* expression in the limb mesenchyme: the distal tip domain, which requires *Gas1* function, and the proximal larger domain, which does not. Second, only this tip region of *Fgf10* expression is responsible for maintenance of the *Fgf8* expression in the entire AER. Although the proximal *Fgf10* expression domain in the mutant extends to the anterior and posterior borders next to the ectoderm, it is not sufficient to maintain *Fgf8* there. Third, *Fgf4*, *9* and *17* expression is present in the mutant, suggesting that either the FGF10 in the proximal region is sufficient to maintain their expression or their expression does not depend on FGF10. One possible mechanism whereby the three *Fgfs* are expressed in the absence of the distal FGF10 is that they are regulated by SHH/ZPA.

The relationship between *Gas1* and the *Fgf8* and *Fgf10* regulatory loop

Gas1 maintains *Fgf10* expression at the tip mesenchyme, either directly or indirectly. *Gas1* is normally expressed in the anterior two-thirds of the limb (Fig. 1H). It is possible that *Gas1* directly controls distal *Fgf10* expression in this region (Fig. 10, model a). In this model, two signals are required to maintain *Fgf10* at the tip, *Gas1* in the mesenchyme and the *Fgf8* in the AER. In a model of indirect control, *Gas1* may help to mediate *Fgf8*'s feedback regulatory loop, which maintains the tip *Fgf10* expression (Fig. 10, model b). In this model, GAS1 is an obligatory component of FGF8 signaling as injection of high doses of FGF8 fails to overcome the *Gas1*$^{-/-}$ phenotype. However, it should be noted that except for their similar limb defects, *Gas1* mutants and *Fgf* mutants do not share any common defects in other tissues outside of the limb (Sun et al., 1999), suggesting a specialized function of *Gas1* in the limb in relation to *Fgf8*. In either model, it is intriguing that the *Fgf10* expression is more affected in the central tip than the anterior region in the *Gas1*$^{-/-}$ limb and that this causes the entire domain of *Fgf8*-AER expression to be lost. Nonetheless, the discovery that *Gas1* in the mesenchyme is an additional

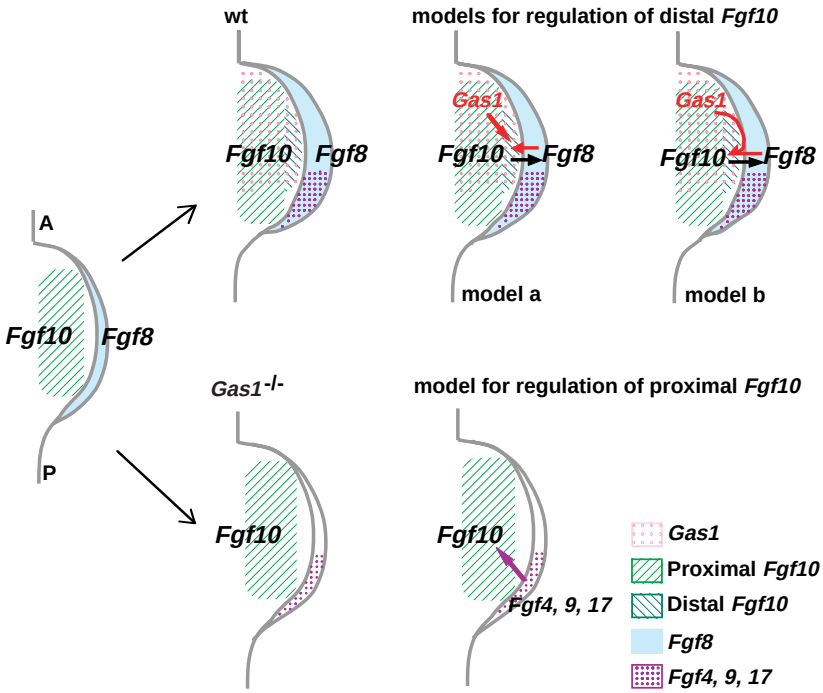

Fig. 10. Proposed models for *Gas1* action and *Fgf10* regulation in the developing limb. At the early phase of limb formation, *Gas1* is not required for *Fgf10*/*Fgf8* expression in the proximal mesenchyme and the AER, respectively (left). In the wild type (wt), *Gas1* is expressed in the anterior two-thirds of the mesenchyme, *Fgf10* in a large contiguous domain of the limb mesenchyme composed of a proximal and a distal domain, and *Fgf8* in the AER. In the *Gas1* mutant, *Fgf10* expression is lacking at the distal domain, *Fgf8* is not maintained and the AER is thinner (bottom panel). Our FGF10 rescue injection data indicate that FGF10 at the distal mesenchyme is continuously required to maintain *Fgf8* expression (black arrow). We propose that *Fgf10* expression in the distal mesenchyme is either directly regulated by *Gas1* and AER *Fgf8*, in parallel (red arrows; model a) or by *Fgf8* in the AER through a pathway that requires *Gas1* activity (converged red arrow; model b). We also propose that the proximal domain of *Fgf10* expression can be maintained (purple arrow) by *Fgf4, 9* and *17* in the posterior AER in the absence of *Fgf8*. *Fgf8* may also contribute to this regulation normally. The color code for each gene expression domain is at the right bottom corner.

component in the regulatory loop between *Fgf10*/*Fgf8* adds a new dimension to this molecular network.

The differences between *Gas1* mutant and *Fgf8* AER-knock-out mutants

The *Gas1* mutant has phenotypes less severe than the two types of *Fgf8*/AER-KO mutants reported. For simplicity, only the forelimb phenotype is discussed. When *Fgf8* is inactivated prior to its expression in the AER (Moon and Capecchi, 2000), there is a severe growth defect and a loss of *Fgf10* expression in the anterior limb. When *Fgf8* is inactivated shortly after its initiation (Lewandoski et al., 2000), the limb defect is milder and the *Fgf10* expression is normal. In both cases, the forelimbs are observably smaller at E10.5 and develop with shortened or missing proximal bones in addition to the autopod defects. In contrast, the *Gas1* mutant's limb size reduction is not measurable prior to E10.5 and the phenotype is restricted to the autopod. One possible explanation is that the *Gas1* mutant loses *Fgf8* expression later and has higher levels of residual FGF8 than both *Fgf8*/AER-KO mutants. The three mutants may thus represent *Fgf8* deficiency at different stages and/or of different levels. Together, these data suggest a progressively diminishing requirement of *Fgf8* activity for the proximal elements during the PD growth and patterning of the limb.

One difference between the *Gas1* and the *Fgf8*/AER-KO mutants is puzzling: high levels of *Fgf4* are activated in the entire AER in both types of *Fgf8*/AER-KO mutants (Moon and Capecchi, 2000; Lewandoski et al., 2000). This does not occur in the *Gas1* mutant. While the precise reason for this difference is unknown, we suggest that activation of compensatory *Fgf4* expression along the entire length of the AER still requires *Fgf10* at the specialized distal tip mesenchyme, which is missing only in the *Gas1* mutant.

Reduced proliferation and digit malformation

Missing phalanges and syndactyly, the phenotype of *Gas1*$^{-/-}$, can also be induced by chemical inhibitors of proliferation, presumably because the autopod elements are most vulnerable as they are formed late (Shubin and Alberch, 1986). The anterior digit condensations appear even later than the posterior ones (Burke and Alberch, 1985), making them more sensitive to growth disruption. The small phalanges and metacarpals in the forelimb of *Hoxd13*$^{-/-}$ mice (Dolle et al., 1993) were attributed to decreased proliferation (Duboule, 1995). We propose that the *Gas1*$^{-/-}$ autopod defects are also a consequence of insufficient precursor mesenchyme generated earlier, thereby causing delayed chondrogenesis and small condensation sizes. The anterior digit defects may thus be due to depletion of a smaller pool of mesenchymal cells by early condensing posterior elements. Since the alterations of the proliferation and PCD patterns in the mutant do not strictly correlate with *Gas1* expression, we suggest that they reflect a secondary consequence of the heterochrony of the mutant limb caused by the deregulation of *Fgf8*. The loss of *Fgf8* expression may also account for reduced PCD at E11.5 (Montero et al., 2001). Finally, the relatively normal patterns of the condensations and expression of *Bmp2*, *Bmp4*, *Bmp7*, *BmpRIB*, *Ihh*, and *PTHrP* in the *Gas1*$^{-/-}$ limb further argue for a defect in early mesenchymal mass rather than a disruption in patterning or bone growth per se. As the chondrogenic growth regulatory network appears relatively normal, this may explain the post-natal compensatory growth of the mutant autopod elements.

We are in debt to Dr Lee Niswander for her encouragement and insights to help us to complete this project, and her tireless effort to correct the manuscript. We also thank Drs A. Fire, D. Koshland and a member of the Tabin lab for critical reading of the manuscript. This work is supported by the Beckman Foundation, the Dammon-Runyon Cancer Research Fund and an NIH grant (R01-HD 35596).

REFERENCES

Ahn, K., Mishina, Y., Hanks, M. C., Behringer, R. R. and Crenshaw, E. B. 3rd (2001). BMPR-IA signaling is required for the formation of the apical ectodermal ridge and dorsal-ventral patterning of the limb. *Development* **128**, 4449-4461.

Bancroft, J. D. and Cook, H. C. (1994). *Manual of Histological Techniques and their Diagnostic Application.* London: Churchill Livingstone.

Burke, A. C. and Alberch, P. (1985). The development and homology of the chelonian carpus and tarsus. *J. Morphol*. **186**, 119-132.

Charite, J., de Graaff, W., Shen, S. and Deschamps, J. (1994). Ectopic expression of *Hoxb-8* causes duplication of the ZPA in the forelimb and homeotic transformation of axial structures. *Cell* **78**, 589-601.

Chiang, C., Litingtung, Y., Harris, M. P., Simandl, B. K., Li, Y., Beachy, P. A. and Fallon, J. F. (2001). Manifestation of the limb prepattern: limb development in the absence of sonic hedgehog function. *Dev. Biol*. **236**, 421-435.

Crossley, P. H., Minowada, G., MacArthur, C. A. and Martin, G. R. (1996). Roles for FGF8 in the induction, initiation, and maintenance of chick limb development. *Cell* **84**, 127-136.

Del Sal, G., Ruaro, E. M., Philipson, L. and Schneider, C. (1992). The growth arrest-specific gene, gas1, is involved in growth suppression. *Cell* **70**, 595-607.

Dolle, P., Dierich, A., Lemeur, M., Schinnang, T., Schuhbaur, B., Chambon, P. and Duboule, D. (1993). Disruption of the *Hoxd13* gene induces localized heterochrony leading to mice with neoteric limbs. *Cell* **75**, 432-441.

Duboule, D. (1995). Vertebrate *Hox* genes and proliferation: An alternative pathway to homeosis? *Curr. Opin. Genet. Dev.* **5**, 525-528.

Echelard, Y., Epstein, D. J., St-Jacques, B., Shen, L., Mohler, J., McMahon, J. A. and McMahon, A. P. (1993). Sonic hedgehog, a member of a family of putative signaling molecules, is implicated in the regulation on CNS polarity. *Cell* **75**, 1417-1430.

Erlebacher, A., Filvaroff, E., Gitelman, S. and Derynck, R. (1995). Toward a molecular understanding of skeletal development. *Cell* **80**, 371-378.

Fan, C.-M. and Tessier-Lavigne, M. (1994). Patterning of mammalian somites by surface ectoderm and notochord: Evidence for sclerotome induction by a hedgehog homolog. *Cell* **79**, 1175-1186.

Galceran, J., Farinas, I., Depew, M. J., Clevers, H. and Grosschedl, R. (1999). *Wnt3a*$^{-/-}$ like phenotype and limb deficiency in *Lef1*$^{-/-}$ *Tcf1*$^{-/-}$ mice. *Genes Dev.* **13**, 709-717.

Ganan, Y., Macias, D., Duterque-Coquillaud, M., Ros, M. A. and Hurle, J. M. (1996). Role of TGFs and BMPs as signals controlling the position of the digits and the areas of cell death in the developing chick limb autopod. *Development* **122**, 2349-2357.

Harrison, R. G. (1921). On relations of symmetry in transplanted limbs. *J. Exp. Zool.* **32**, 1-136.

Hinchliffe, J. R. (1982). Cell death in vertebrate limb morphogenesis, in *Progress in Anatomy.* Vol. 2 (ed. Harrison, R. J. and Navaratnam V.), pp. 113-126. Cambridge, UK: Cambridge University Press.

Hinchliffe, J. R. and Griffiths, P. J. (1983). The prechondrogenic patterns in tetrapod limb development and their phylogenetic significance, in *Development and Evolution* (ed. Goodwin, B. C., Hilder, N. H. and Wylie, C. C.), pp. 99-121. Cambridge, UK: Cambridge University Press,

Hogan, B. L. M. (1996). Bone morphogenetic proteins: multifunctional regulators of vertebrate development. *Genes Dev*. **10**, 1580-1594.

Hui, C., Slusarski, D., Platt, K. A., Holmgren, R. and Joyner, A. L. (1994). Expression of three mouse homologies of *Drosohila* segment polarity gene *cubitus interruptus, Gli, Gli-2,* and *Gli-3*. In ectoderm- and mesoderm-derived tissues suggests multiple roles during postimplantation development. *Dev. Biol.* **162**, 402-413.

Hurle, J. M., Ros, M. A., Garcia-Martinez, V., Mascias, D. and Ganan, Y. (1996). Cell death in the embryonic developing limb. *Scan. Micro*. **9**, 519-534.

Johnson, R. L. and Tabin, C. J. (1997). Molecular models for vertebrate limb development. *Cell* **90**, 979-990.

Kawakami, Y., Capdevila, J., Buscher, D., Itoh, T., Rodriguez-Esteban, C. and Belmonte, J. C. I. (2001). WNT signals control FGF-dependent limb initiation and AER induction in the chick embryo. *Cell* **104**, 891-900.

Lee, C. S. and Fan, C.-M. (2001). Embryonic expression patterns of mouse and chick *Gas1* genes. *Mech. Dev.* **101**, 293-297.

Lee, C. S., Buttitta, L. and Fan, C.-M. (2001a). Evidence that the WNT-inducible growth arrest specific gene 1 encodes an antagonist of sonic hedgehog signaling in the somite. *Proc. Natl. Acad. Sci., USA* **98**, 11347-11352.

Lee, C. S., May, N. R. and Fan, C.-M. (2001b). Conversion of the ventral retinal pigmented epithelium to neural retina in the *Gas1* mutant mice. *Dev. Biol.* **236**, 17-29.

Lee, K. K., Leung, A. K., Tang, M. K., Cai, D. Q., Schneider, C., Brancolini, C. and Chow, P. H. (2001c). Functions of the growth arrest specific 1 gene in the development of the mouse embryo. *Dev. Biol.* **234**, 188-203.

Lewandoski, M., Sun, X. and Martin, G. R. (2000). *Fgf8* signaling from the AER is essential for normal limb development. *Nat. Genet* **26**, 460-463.

Liu, Y., May, N. R. and Fan, C.-M. (2001). *Gas1* is a positive regulator for the proliferation of the cerebellum. *Dev. Biol.* **236**, 30-45.

Mahmood, R., Bresnick, J., Hornbruch, A., Mahony, C., Morton, N., Colquhoun, K., Martin, P., Lumsden, A., Dickson, C. and Mason, I. (1995). A role for FGF-8 in the initiation and maintenance of vertebrate limb bud outgrowth. *Curr. Biol.* **5**, 797-806.

Marigo, V., Scott, M. P., Johnson, R. L., Goodrich, L. V. and Tabin, C. J. (1996). Conservation in Hedgehog signaling-induction of a chicken *Patched* homologue by *Sonic hedgehog* in the developing limb. *Development* **122**, 1225-1233.

Martin, G. R. (1998). The roles of FGFs in the early development of vertebrate limbs. *Genes Dev*. **12**, 1571-1586.

Min, H., Danilenko, D. M., Scully, S. A., Bolon, B., Ring, B. D., Tarpley, J. E., DeRose, M. and Simonet, W. S. (1998) *Fgf-10* is required for both limb and lung development and exhibits striking functional similarity to *Drosophila branchless*. *Genes Dev.* **12**, 3156-3161.

Montero, J. A., Ganan, Y., Macias, D., Rodriguez-Leon, J., Sanz-Ezquerro, J. J., Merino, R., Chimal-Monroy, J., Nieto, M. A. and Hurle, J. M. (2001). Role of FGFs in the control of programmed cell death during limb development. *Development* **128**, 2075-2084.

Moon, A. M. and Capecchi, M. R. (2000). *Fgf8* is required for outgrowth and patterning of the limbs. *Nat Genet* **26**, 455-459.

Ohuchi, H., Nakagawa, T., Yamamoto, A., Araga, A., Ohata, T., Ishimaru, Y., Yoshioka, H., Kuwana, T., Nohno, T., Yamasaki, M., Itoh, N. and Noji, S. (1997). The mesenchymal factor, FGF10, initiates and maintains the outgrowth of the chick limb bud through interaction with FGF8, an apical ectodermal factor. *Development* **124**, 2235-2244.

Pizette, S. and Niswander, L. (1999). BMPs negatively regulate structure and function of the limb apical ectodermal ridge. *Development* **126**, 883-894.

Pizette, S., Abate-Shen, C. and Niswander, L. (2001). BMP controls proximodistal outgrowth, via induction of the apical ectodermal ridge, and dorsoventral patterning in the vertebrate limb. *Development* **128**, 4463-4474.

Qu, S., Niswender, K., Ji, Q., van der Meer, R., Keeney, D., Magunson, M. and Wisdom, R. (1997). Polydactyly and ectopic ZPA formation in *Alx4* mutant mice. *Development* **124**, 3999-4008.

Riddle, R. D., Johnson, R. L., Laufer, E. and Tabin, C. (1993). Sonic hedgehog mediates the polarizing activity of the ZPA. *Cell* **75**, 1401-1416.

Saunders, J. W., Jr (1948). The proximo-distal sequence of origin of the parts of the chick wing and the role of the ectoderm. *J. Exp. Zool.* **108**, 363-404.

Sekine, K., Ohiuchi, H., Fujiwara, M., Yamasaki, M., Yoshizawa, Y., Sato, T., Yagishita, N., Matsui, D., Koga, Y., Itoh, N. and Kato, S. (1999). *Fgf10* is essential for limb and lung formation. *Nat. Genet.* **21**, 138-141.

Shubin, N. H. and Alberch, P. (1986). A morphogenetic approach to the origin and basic organization of the tetrapod limb. *Evol. Biol.* **20**, 319-387.

St-Jacques, B., Hammerschmidt, M. and McMahon, A. P. (1999). Indian hedgehog signaling regulates proliferation and differentiation of chondrocytes and is essential for bone formation. *Genes Dev.* **13**, 2072-2086.

Stebel, M., Vatta, P., Ruaro, M. E., del Sal, G., Parton, R. G. and Schneider, C. (2000). The growth suppressing gas1 product is a GPI-linked protein. *FEBS Lett.* **481**, 152-158.

Stocum, D. and Fallon, J. (1982). Control of pattern formation in urodele limb ontogeny: A review and hypothesis. *J. Embryol. Exp. Morphol.* **69**, 7-36.

Sun, X., Meyers, E. N., Lewandoski, M. and Martin, G. R. (1999). Targeted disruption of *Fgf8* causes failure of cell migration in the gastrulating mouse embryo. *Genes Dev.* **13**, 1834-1846.

Sun, X., Mariani, F. V. and Martin, G. R. (2002). Functions of FGF signalling from the apical ectodermal ridge in limb development. *Nature* **418**, 501-508.

Vogel, A., Rodriguez, C. and Izpisua-Belmonte, J. C. (1996). Involvement of FGF-8 in initiation, outgrowth and patterning of the vertebrate limb. *Development* **122**, 1737-1750.

Vortkamp, A., Lee, K., Lanske, B., Segre, G. V., Kronenberg, H. M. and Tabin, C. J. (1996). Regulation of rate of cartilage differentiation by Indian hedgehog and PTH-related protein. *Science* **273**, 613-622.

Wilkinson, D. G. (1992) *In Situ Hybridization: A Practical Approach.* Oxford: Oxford University Press.

Zou, H., Wieser, R., Massague, J. and Niswander, L. (1997). Distinct roles of type I bone morphogenetic protein receptors in the formation and differentiation of cartilage. *Genes Dev.* **11**, 2191-2203.

Zuniga, A., Haramis, A.-P. G., McMahon, A. P. and Zeller, R. (1999). Signal relay by BMP antagonism controls the SHH/FGF4 feedback loop in vertebrate limb buds. *Nature* **401**, 598-602.

Zwilling, E. (1961). Limb morphogenesis. *Adv. Morphogen.* **1**, 301-330.